



April–September minimum temperature reconstruction based on *Sabina tibetica* ring-width chronology in the central eastern Tibetan Plateau, China

Teng Li¹ · Jianfeng Peng² · Tsun Fung Au^{3,4} · Jinbao Li^{5,6}

Received: 21 June 2023 / Accepted: 5 July 2023
© The Author(s) 2024

Abstract Minimum temperatures have remarkable impacts on tree growth at high-elevation sites on the Tibetan Plateau, but the shortage of long-term and high-resolution paleoclimate records inhibits understanding of recent minimum temperature anomalies. In this study, a warm season (April–September) reconstruction is presented for the past 467 years (1550–2016) based on *Sabina tibetica* ring-width chronology on the Lianbaoyeze Mountain of the central eastern Tibetan Plateau. Eight warm periods and eight cold periods were identified. Long-term minimum temperature variations revealed a high degree of coherence with nearby reconstructions. Spatial correlations between our reconstruction and global sea surface temperatures suggest that warm season minimum temperature anomalies in the central eastern Tibetan Plateau were strongly influenced by large-scale ocean atmospheric circulations, such as the El

Niño–Southern Oscillation and the Atlantic Multidecadal Oscillation.

Keywords Tree-ring analysis · *Sabina tibetica* · Minimum temperatures · Central eastern Tibetan Plateau · Climate change

Introduction

Tree growth is a complex biological process, whereas climate is a key determinant of tree adaptation and productivity. IPCC (2021) reported that global surface temperatures during the past decade (2011–2020) were 1.1 °C above those during 1850–1900. Among all the factors that affect tree growth, temperature is the most critical in high latitudes and alpine regions. As a result, tree-ring records of high elevation sites often bear important imprints of temperature variabilities.

Tree-ring parameters provide an opportunity to evaluate past climate changes when instrument observations are unavailable (Davi et al. 2015; Asad et al. 2016; Zhang 2015; Zhang et al. 2019, 2020). As an annual climate proxy, tree rings have been widely used in climate reconstructions at local to global scales (Esper et al. 2002; Mann et al. 2008;

Project funding: This research was funded by the National Key Research and Development Program of China (No. 2018YFA0605601), Hong Kong Research Grants Council (No. 106220169), and the National Natural Science Foundation of China (No. 42105155, 41671042, and 42077417), and the National Geographic Society (No. EC-95776R-22).

The online version is available at <http://www.springerlink.com>

Corresponding editor: Tao Xu.

✉ Teng Li
liteng@gzhu.edu.cn

¹ School of Geography and Remote Sensing, Guangzhou University, Guangzhou 510006, People's Republic of China

² College of Geography and Environmental Science, Henan University, Kaifeng 475004, People's Republic of China

³ Institute for Global Change Biology, School for Environment and Sustainability, University of Michigan, Ann Arbor, MI, USA

⁴ Department of Ecology and Evolutionary Biology, University of Michigan, Ann Arbor, MI, USA

⁵ Department of Geography, University of Hong Kong, Hong Kong SAR, People's Republic of China

⁶ HKU Shenzhen Institute of Research and Innovation, Shenzhen 518057, People's Republic of China

Cook et al. 2010; Gou et al. 2013; Fang et al. 2014; Li et al. 2014a; Wilson et al. 2016; Sun et al. 2018; Chen et al. 2019). Dendroclimatological research has developed rapidly in China in recent decades (Shao et al. 2010; Yang et al. 2014; Zhang et al. 2015; Liu et al. 2017a; Yang et al. 2017; Fan et al. 2019; Yu and Liu 2020; Jiao et al. 2022). Numerous studies have reconstructed temperature, precipitation, moisture, and streamflow across China (Shao et al. 2005; Liang et al. 2009; Liu et al. 2009, 2017b; Bao et al. 2012; Peng and Liu 2013; Zhang et al. 2014a; Chen et al. 2016; Fang et al. 2017; Li et al. 2017; Shi et al. 2017; Wang et al. 2019). In particular, tree-ring studies in the eastern Tibetan Plateau started in the 1990s (Shao and Fan 1999), but most were concerned with the reconstruction of winter or annual temperatures (Wu et al. 2005; Song et al. 2007; Yu et al. 2012; Li et al. 2014b, 2015a, 2015b; Xiao et al. 2015; Yin et al. 2015; Zhu et al. 2016) or the variability of drought (Deng et al. 2016, 2017). Growing season temperature reconstructions are relatively rare in the eastern Tibetan Plateau, and there is a need to expand the tree-ring coverage, especially for the growing season minimum temperatures.

The central eastern Tibetan Plateau has an average altitude of 4000 m a.s.l. It is characterized by complex topography, thin air with low oxygen levels, and high annual solar radiation (Hu and Zeng 2003). Abundant sunshine makes

up, to some extent, for heat loss at high altitudes and cold weather. As a result, trees can grow to a higher elevation, which makes minimum temperatures a key limiting factor on tree growth.

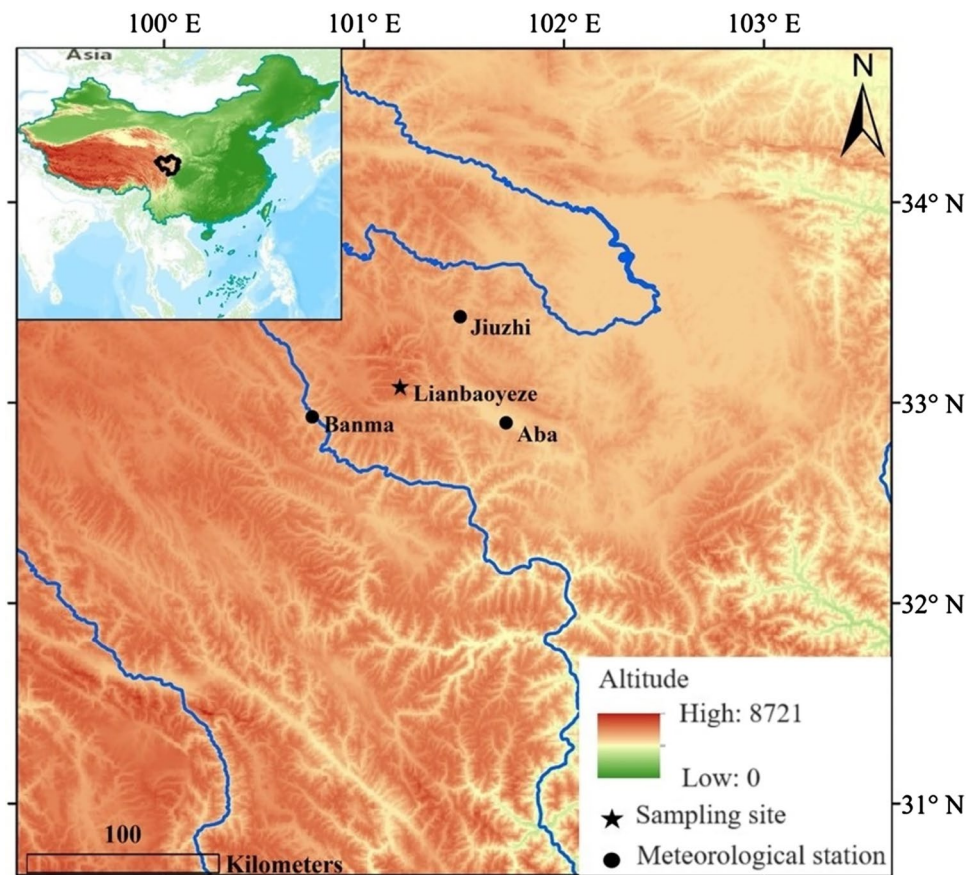
The objective of this study was to reconstruct growing season minimum temperatures based on tree-ring analysis of *Sabina tibetica* Kom. collected from the Lianbaoyeze Mountain in central eastern Tibetan Plateau and to investigate the long-term variations of minimum temperatures and their potential climate driving factors.

Materials and methods

Study region

The Lianbaoyeze Mountain (33.08° N, 101.18° E) belongs to the southern branch of the Bayan Har Mountains and is located in the northwest of Aba County of Sichuan Province, bordering Jiuzhi County and Banma County of Qinghai Province. The average elevation is over 4000 m and the highest peak is 5141 m a.s.l. Based on nearby meteorological records from the China Meteorological Data Service Centre (<http://data.cma.cn/>), the annual average temperature is 3.3 °C, annual total rainfall 712 mm, and annual total

Fig. 1 Study area showing the sampling site (star) and nearby meteorological stations (circles)



sunshine 2383 h. *S. tibetica* is mainly distributed on sunny slopes from 2800 to 4500 m a.s.l. (Fig. 1).

Tree-ring data

A total of 83 cores from 40 trees (2–3 cores ind⁻¹) of *S. tibetica* were collected from living and dead trees in 2017. Following standard dendrochronological procedure (Stokes and Smiley 1968), the cores were glued to wooden mounts, air dried, and sanded with fine sandpaper until the ring boundaries were clearly seen under a microscope. Rings were visually cross-dated, and then measured using the Velmex measuring system with a precision of 0.001 mm. The cross-dating and ring-width measurements were checked using the COFECHA program (Holmes 1983) for quality control.

The cross-dated ring-width sequences were conservatively detrended using negative exponential or linear curves of any slope (Cook and Kairiukstis 1990). The tree-ring indices were calculated as residuals after performing an adaptive power transformation, which stabilizes the variance in heteroscedastic raw ring-width series (Cook and Peters 1997). The tree-ring indices were merged to generate tree-ring chronologies by ARSTAN program (Cook and Holmes

1986) and a standard chronology used (Fig. 2). The reliable period of the chronology was determined by the expressed population signal (EPS) threshold value of 0.85 (Wigley et al. 1984), a commonly used criterion to assess whether a chronology is statistically reliable for climate reconstruction (Cook and Kairiukstis 1990).

Climate data

Monthly climate data spanning 1963–2016 were collected from the Jiuzhi meteorological station (31° N, 102° 12' E, 2370 m a.s.l.). Climate factors include monthly mean (T_{mean}), maximum (T_{max}), minimum (T_{min}) temperatures, and monthly total precipitation (P) (Fig. 3). In addition, the Climatic Research Unit (CRU) TS4.04 temperature dataset (Harris et al. 2020) and Hadley Centre sea surface temperature dataset (HadISST1; Rayner et al. 2003) were adopted for spatial correlation analyses.

Statistical analysis

Pearson's correlation analyses between standard chronology and regional climate factors (T_{mean} , T_{max} , T_{min} and P) from

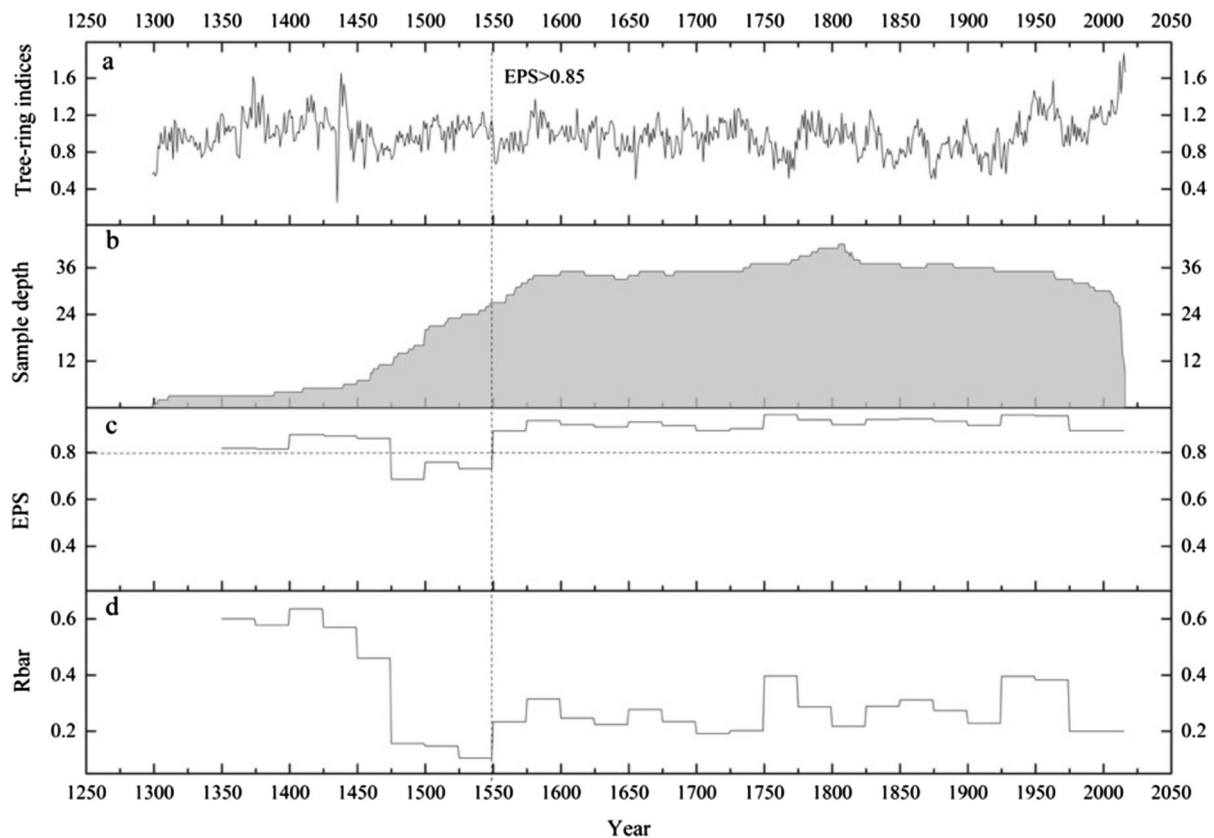


Fig. 2 **a** Tree-ring width chronology developed from *S. tibetica*, **b** Sample depth, **c** Running EPS, **d** Running Rbar; vertical dashed line denotes EPS > 0.85

Fig. 3 Monthly mean (T_{mean}), maximum (T_{max}), minimum (T_{min}) temperatures and monthly total precipitation (P) from the Jiuzhi meteorological data (1963–2016)

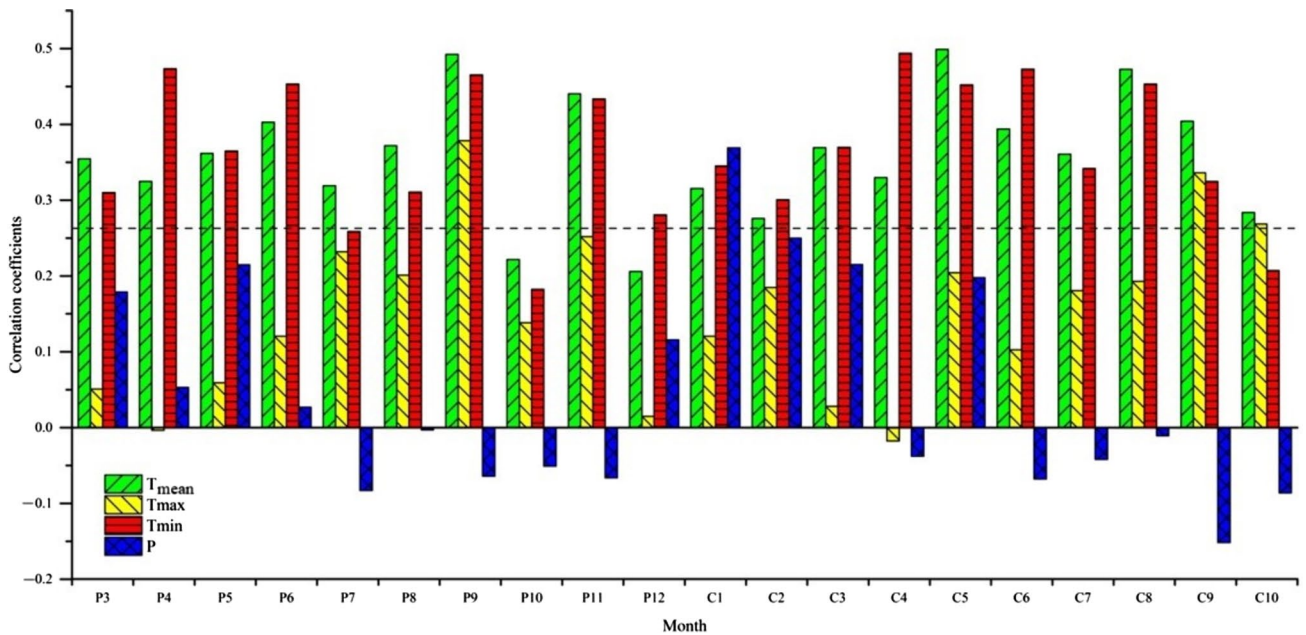
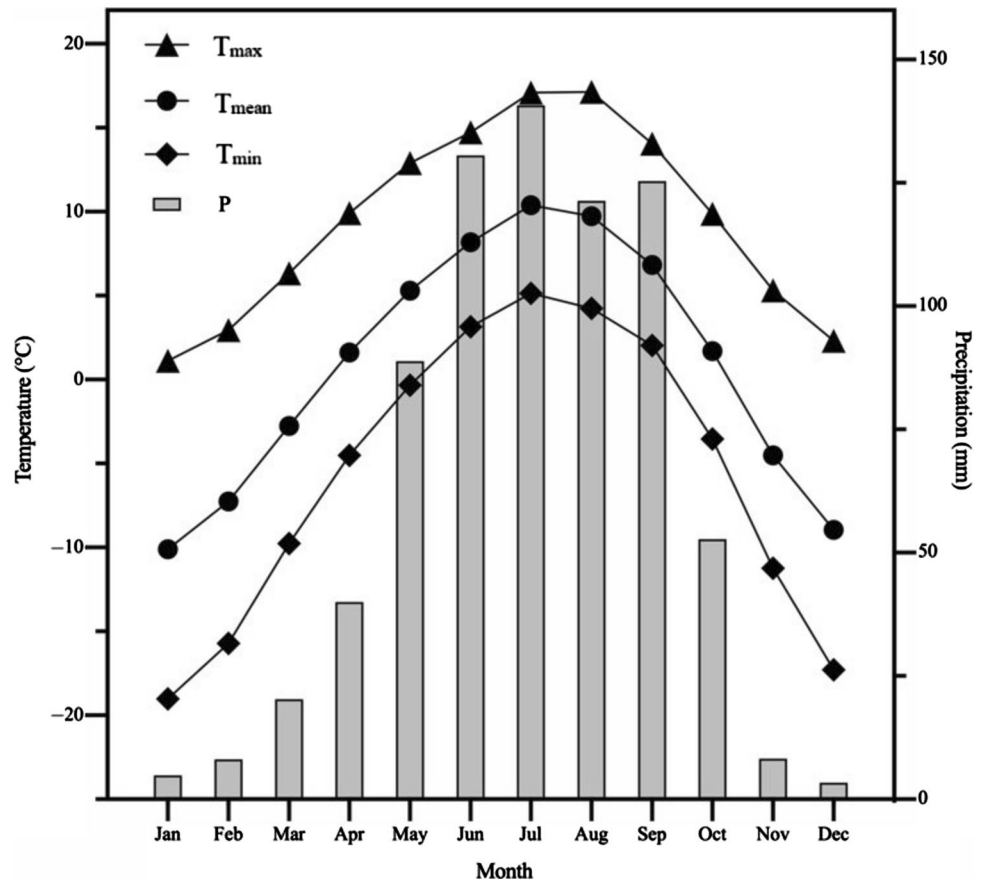


Fig. 4 Correlations of ring-width chronology of *S. tibetica* with monthly climate factors (T_{mean} , T_{max} , T_{min} and P) from the previous March to the current October over 1963–2016; horizontal dashed line denotes the 0.05 significance level

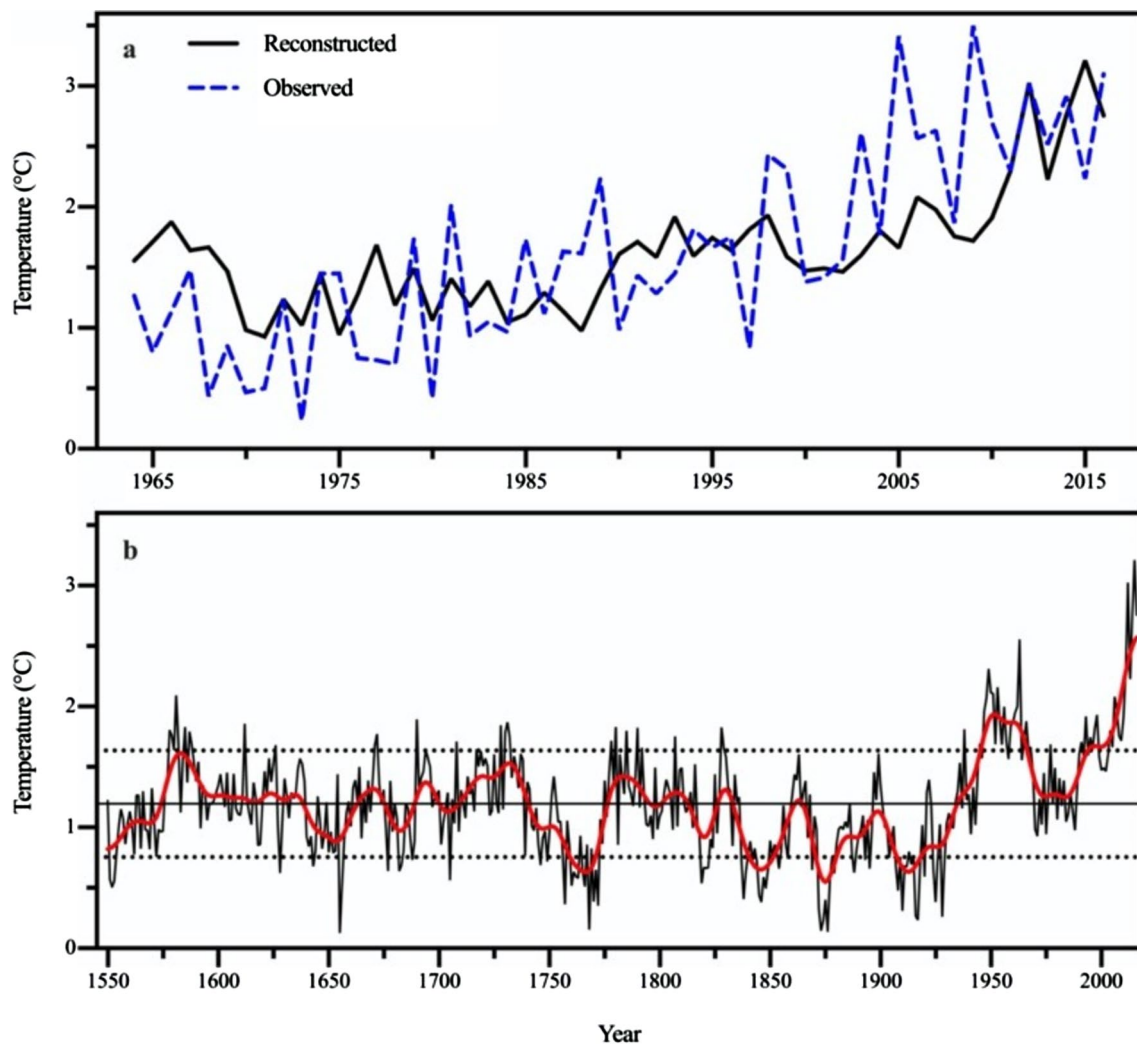


Fig. 5 **a** Comparison of observed (dash line) and reconstructed (solid line) T_{\min} 1964–2016, **b** The reconstructed T_{\min} and its 21-year low-pass filter (thick line) 1550–2016

the previous March to the current October were performed over 1963–2016. Based on the results of the climate-growth relationship, the dominant limiting factor was selected for reconstruction with a simple linear regression method (Fritts 1976; Cook and Kairiukstis 1990). The leave-one-out cross-validation (LOOCV) method was employed to test the robustness of the reconstruction model because of the short common period between tree-ring width chronology and meteorological records (Michaelsen 1987). A positive value of the reduction of error (RE) denotes the fidelity of reconstruction model.

Multi-taper method (MTM; Mann and Lees 1996) and wavelet analysis (Torrence and Compo 1998) were used to explore periodic variations of the reconstruction. Spatial correlation analyses were performed between the actual and reconstructed series and CRU TS4.04 temperature dataset to reveal the spatial representativeness of the reconstruction.

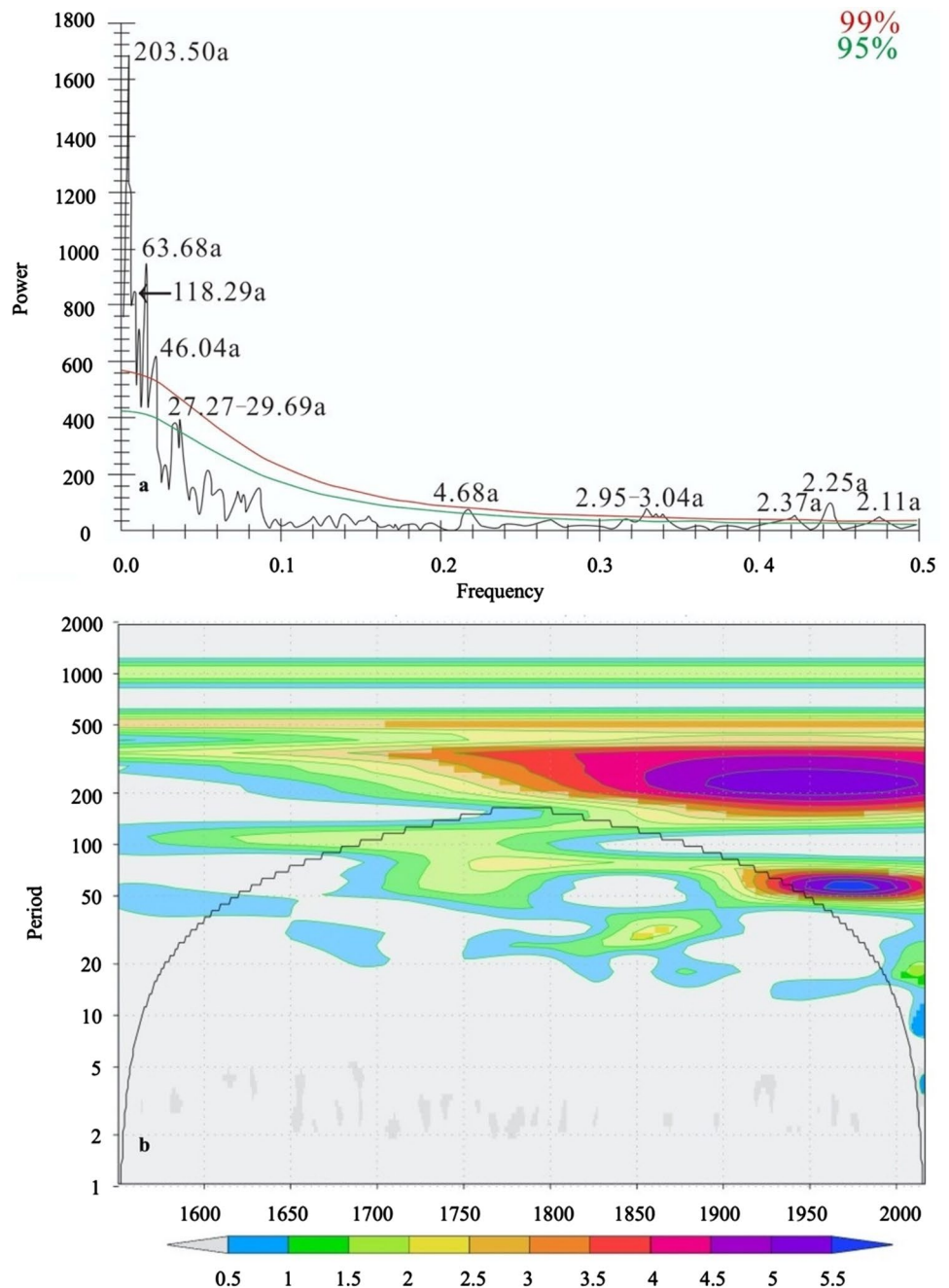
In addition, spatial correlations between the reconstructed series and HadSST1 SST dataset were calculated to determine the impact of global SSTs on climate variability in the study area. Spatial correlations were performed using the KNMI Climate Explorer (<http://www.knmi.nl>).

Results

Climate-growth relationships

A ring-width chronology of *S. tibetica* was developed which spans 1299–2016 with a mean segment length of 379.3 years. The reliable portion of the chronology covers 1550–2016 based on the EPS threshold of 0.85 (Fig. 2). The R_{bar} of the reliable chronology ranges from 0.20 to 0.40, with an average value of 0.27 (Fig. 2). Based on the statistics

Fig. 6 a MTM spectral results of the reconstructed T_{\min} 1550–2016. The red and green lines denote 0.01 and 0.05 significance level, respectively; **b** Wavelet analysis of the reconstructed T_{\min} 1550–2016. The black line indicates the cone of influence beyond which the edge effect may contort the results. Shading denotes the 0.05 significance level



of EPS and Rbar, the chronology holds strong and stable climate signals and is suitable for dendroclimatic studies.

Growth of *S. tibetica* was positively correlated with almost all temperature factors (Fig. 4). It had significant positive correlations with T_{mean} and T_{min} in the previous March to September, previous November, and the current January to October. It also had significant positive correlations with T_{max} in the previous September and in the current September–October. At the same time, growth of *S. tibetica* showed a weak relationship with precipitation, although there was a significant positive correlation in the current January. These

results indicate that T_{mean} and T_{min} were the most important limiting factors affecting growth of *S. tibetica* in the central eastern Tibetan Plateau.

Regional T_{min} reconstruction

Based on the climate-growth relationship, a linear regression model between ring-width chronology and warm season T_{min} was developed for reconstruction (Cook and Kairiukstis 1990). The reconstruction explained 37.8% (36.6% after adjusting for the degree of freedom) of the T_{min} variance

from 1964 to 2016. A comparison between the observed and reconstructed T_{\min} showed good consistency during 1964–2016 (Fig. 5a). The LOOCV generated reconstruction had a significant positive correlation with the observed data ($r=0.58$, $p<0.01$). The positive RE value (0.29) and low root mean squared error value (0.66) suggest that the reconstruction model is robust. Therefore, the warm season T_{\min} for the central eastern Tibetan Plateau was reconstructed for the past 467 years based on the linear regression model (Fig. 5b).

The reconstructed T_{\min} ranged from 0.13 to 3.21 °C with a mean of 1.19 °C and a standardized deviation (σ) of 0.44 °C over the past 467 years (Fig. 5b). An extremely high temperature was defined as above 1.63 °C (mean + 1σ) and an extremely low temperature as below 0.75 °C (mean - 1σ). Therefore, there were 70 extremely high temperature years and 69 extremely low temperature years, which accounted for 14.99% and 14.78% of the past 467 years, respectively. Among them, the top ten warmest years were 2015, 2012, 2014, 2016, 1963, 1949, 2011, 2013, 1953 and 1950, ranging from 2.12 to 3.21 °C, and the top ten coldest years were 1655, 1876, 1873, 1768, 1874, 1917, 1928, 1916, 1910 and 1872, ranging from 0.13 to 0.33 °C. Based on the 21-year low-pass filter of the reconstruction, there were 8 warm periods (1575–1638, 1663–1675, 1689–1700, 1709–1740, 1777–1795, 1801–1812, 1827–1833, 1935–2016) and 8 cold periods (1550–1574, 1639–1662, 1676–1688, 1701–1708, 1741–1776, 1796–1800, 1813–1826, 1834–1934) in the past 467 years.

Periodic variations of the reconstructed T_{\min}

The MTM spectral analysis showed that the reconstructed T_{\min} had inter-annual (2.11a, 2.25a, 2.37a, 2.95–3.04a, 4.68a), multi-decadal (46.04a, 63.68a), centennial (118.29a) and bicentennial (203.5a) cycles significant at 0.01 significance level (Fig. 6a). In addition, a multi-decadal periodicity (27.27–29.69a) at the 0.05 significance level was also found. Wavelet analysis indicated that multi-decadal and bicentennial cycles were the main periodicities of the T_{\min} series 1550–2016 (Fig. 6b). The multi-decadal cycles were most pronounced during the 1880–2010s, while the bicentennial cycles were most pronounced during the 1700–2010s.

Discussion

Climate-growth relationships

According to the correlations between ring-width chronology and climatic factors, warm season T_{\min} is the dominant limiting factor on tree growth on the central eastern Tibetan Plateau. Numerous studies have revealed that tree growth at high-altitude sites reflect minimum temperature signals on the eastern Tibetan Plateau (Gou et al. 2007; Liang et al. 2009; He et al. 2014; Shi et al. 2015; Li and Li 2017; Huang et al. 2019; Li et al. 2021). T_{\min} could influence cell division in the cambium and the enlargement of tracheids during the growing season (Deslauriers et al. 2003). Low air temperatures at night reduce soil temperatures and may constrain root growth and water uptake

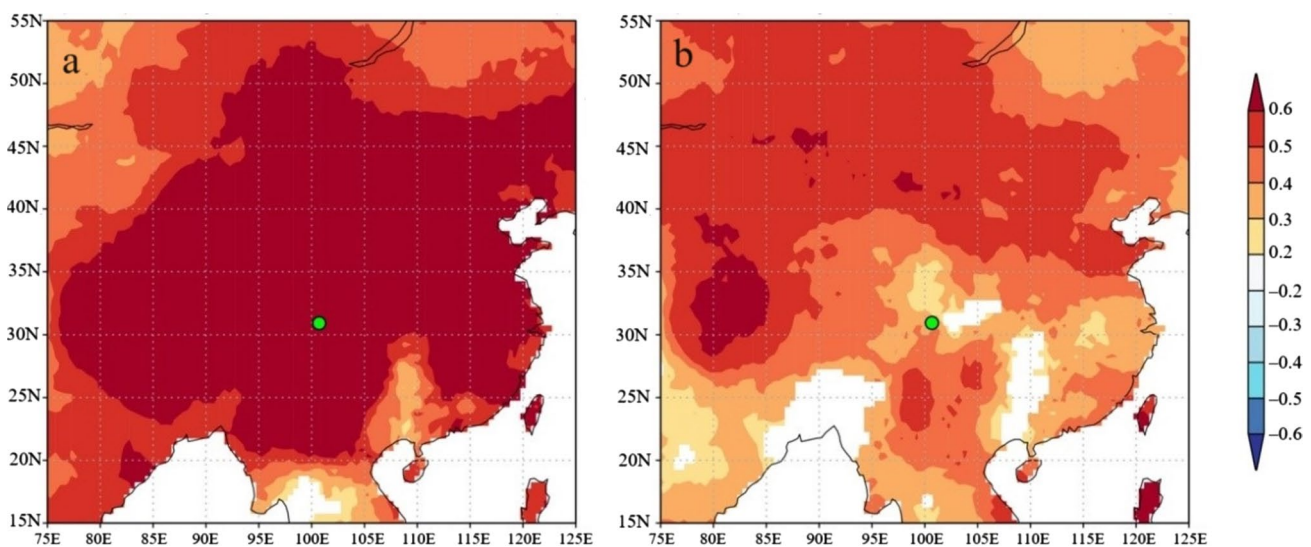


Fig. 7 Spatial correlations of **a** observed and **b** reconstructed T_{\min} with CRU TS4.04 T_{\min} during 1964–2016

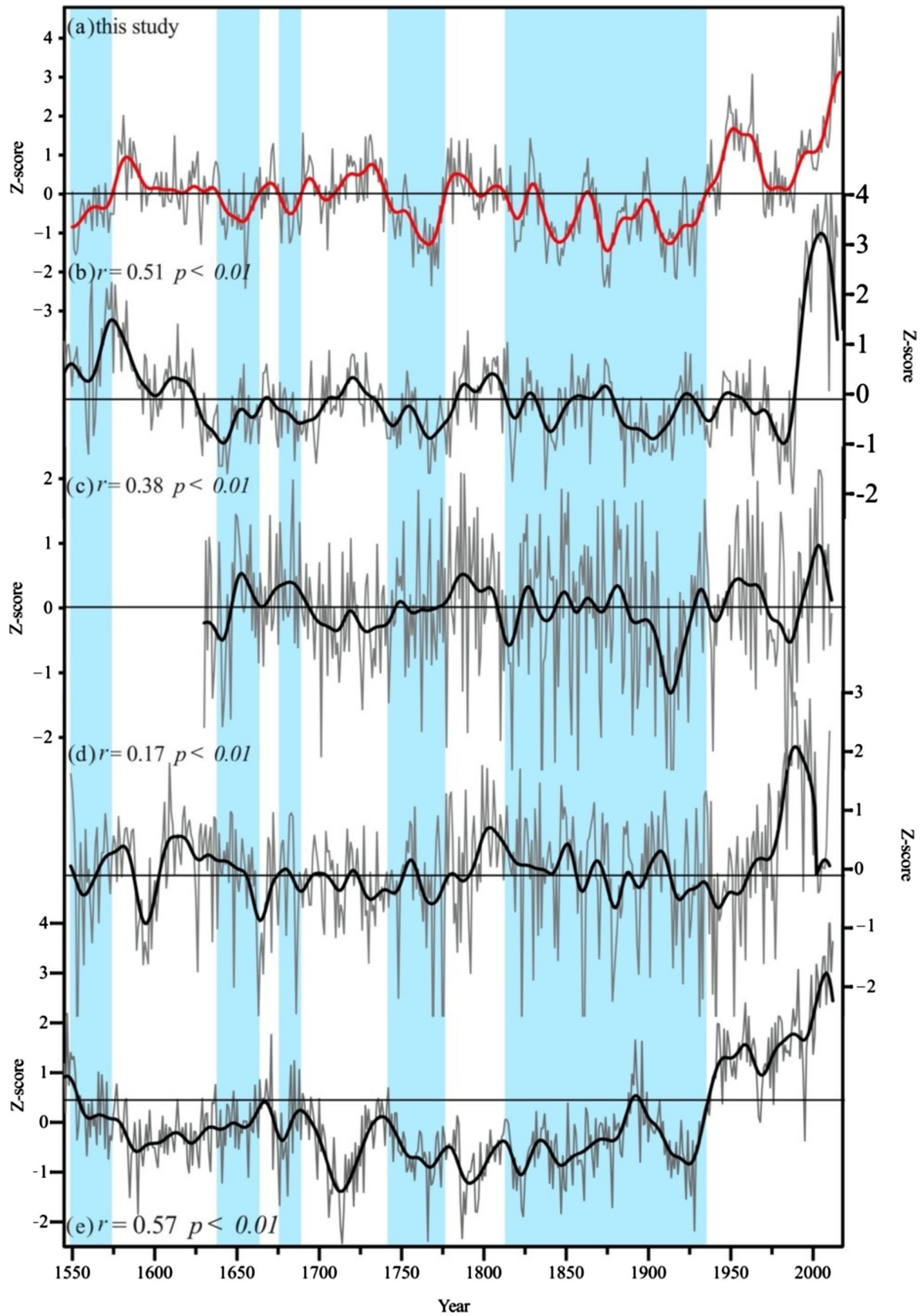


Fig. 8 Comparison of T_{\min} reconstruction in this study with T_{\min} reconstructions from other studies on the Tibetan Plateau. **a** the T_{\min} reconstruction in this study, **b** the previous April to current March T_{\min} reconstruction on the east central plateau (Li and Li 2017), **c** August T_{\min} reconstruction on the southeastern plateau (Liang et al. 2016); **d** previous October to current April T_{\min} reconstruction on the northeastern Tibetan Plateau (Gou et al. 2007), and **e** January–August T_{\min} reconstruction on the northern plateau (Zhang et al. 2014b). All reconstructions have been standardized over their common period for direct comparison. In each panel, the grey line represents the raw data and the bold line a 21-year low-pass filter. Light blue shading denotes major cold periods in our reconstruction

(Körner 1999). Therefore, T_{\min} influences tree growth at high-altitude sites by affecting root growth and cambium activity during the growing season.

Spatial representativeness of the reconstruction

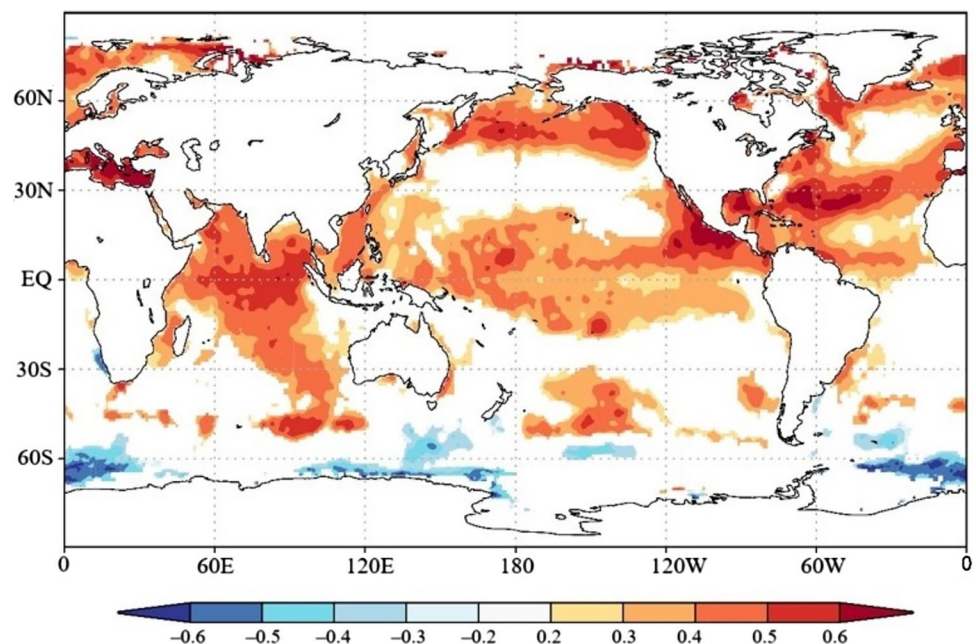
Spatial correlation patterns of the observed and reconstructed T_{\min} with the gridded CRU TS4.04 T_{\min} during 1964–2016 were highly consistent, suggesting that the reconstructed T_{\min} can represent large-scale temperature changes on the plateau (Fig. 7). To further validate the reliability of our reconstruction, four tree-ring based T_{\min} reconstructions from nearby regions were used for comparison: a 564-year previous April to current March reconstruction on the east central plateau (Li and Li 2017), a 382-year August reconstruction on the southeastern plateau (Liang et al. 2016), a 425-year previous October to current April reconstruction on the northeastern plateau (Gou et al. 2007), and a 1343-year January–August reconstruction on the northern plateau (Zhang et al. 2014b). Similar cold and warm periods were found in these T_{\min}

reconstructions (Fig. 8). For example, two major cold periods occurred during the 1740–1770s and 1810–1920s. The cold period of the 1550–1560s in our study was consistent with the previous October to current April variations on the northeastern plateau (Gou et al. 2007), and January–August variations on the northern plateau (Zhang et al. 2014b). The cold periods of the 1640–1650s and in the 1680s in this study were also found in the T_{\min} reconstructions on the east central Tibetan Plateau (Li and Li 2017) and in the north (Zhang et al. 2014b). However, there are some discrepancies between our reconstructions and other T_{\min} reconstructions. For example, the cold period in the 1680s was not captured in the August T_{\min} reconstruction on the southeastern plateau (Liang et al. 2016). The differences among these reconstructions may be related to the growth sensitivity of different tree species under different micro-environments (Classen et al. 2015). Pronounced warming since the 1990s has been observed in all the reconstructions. Overall, the above results indicate that our reconstructions are highly consistent with nearby T_{\min} reconstructions since the 1550s.

Linkages of the T_{\min} variability with global sea surface temperatures (SSTs)

Based on the results of the multi-taper method (MTM) and wavelet analyses, the reconstructed warm season T_{\min} on the eastern plateau has several dominant interannual (2.11a, 2.25a, 2.37a, 2.95–3.04a, 4.68a) and multi-decadal (63.68a) cycles, which are consistent with the 2–7a El Niño–Southern Oscillation (ENSO) cycles and the 60–80a Atlantic Multi-decadal Oscillation (AMO) cycles,

Fig. 9 Spatial correlations of the reconstructed T_{\min} with global April–September averaged sea surface temperatures over 1964–2016



respectively. In addition, our reconstructed T_{\min} series exhibits significant positive correlation ($r=0.54$, $p<0.01$) with the AMO index over 1870–2006 (Mann et al. 2008). Significant positive correlation ($r=0.21$, $p<0.01$) was also found between our T_{\min} reconstruction and the Had-ISST1 Niño3.4 SST index from 1870 to 2006 (Rayner et al. 2003). Spatial correlations between the reconstructed T_{\min} and global SSTs during 1964–2016 showed that there were significant positive correlations with SSTs in the central and northern Pacific Ocean, Indian Ocean, and the North Atlantic Ocean, suggesting that ENSO and AMO played a key role on temperature changes in the central eastern Tibetan Plateau (Fig. 9). Altogether, these results suggest that the T_{\min} variations have a close relationship with ENSO and AMO cycles. Previous studies have shown that climate change on the eastern Tibetan Plateau has been influenced by different large-scale ocean-atmospheric circulations, such as the Asian monsoon, and the ENSO and AMO cycles (Shao and Fan 1999; Song et al. 2007; Duan et al. 2010; Yu et al. 2012; Xiao et al. 2015; Deng et al. 2016; Zhu et al. 2016; Deng et al. 2017; Li and Li 2017; Li et al. 2021), which are consistent with our findings. Nevertheless, further research is needed to reveal the dynamic processes that connect ENSO and AMO cycles with temperature changes on the central eastern Tibetan Plateau.

Conclusion

In this study, a ring-width chronology was developed for *S. tibetica* from the Lianbaoyeze Mountain in the central eastern Tibetan Plateau. Climate-tree growth analysis showed that growth of *S. tibetica* was mostly limited by the warm season (April–September) minimum temperatures. Based on this relationship, we reconstructed warm season T_{\min} for the past 467 years, which revealed 8 warm periods (1575–1638, 1663–1675, 1689–1700, 1709–1740, 1777–1795, 1801–1812, 1827–1833, 1935–2016) and 8 cold periods (1550–1574, 1639–1662, 1676–1688, 1701–1708, 1741–1776, 1796–1800, 1813–1826, 1834–1934). Spatial correlations and comparisons with other T_{\min} reconstructions on the plateau confirmed that our reconstruction represented large-scale T_{\min} variations on the Tibetan Plateau. Further analyses indicated that temperature changes in central eastern plateau may be affected by large-scale ocean-atmospheric circulations such as ENSO and AMO. Future research should develop a larger tree-ring network with longer chronologies for the central eastern Tibetan Plateau to help better understand long-term associations of regional climates with large-scale ocean-atmospheric circulations.

Open Access This article is licensed under a Creative Commons Attribution 4.0 International License, which permits use, sharing, adaptation, distribution and reproduction in any medium or format, as long as you give appropriate credit to the original author(s) and the source, provide a link to the Creative Commons licence, and indicate if changes were made. The images or other third party material in this article are included in the article's Creative Commons licence, unless indicated otherwise in a credit line to the material. If material is not included in the article's Creative Commons licence and your intended use is not permitted by statutory regulation or exceeds the permitted use, you will need to obtain permission directly from the copyright holder. To view a copy of this licence, visit <http://creativecommons.org/licenses/by/4.0/>.

References

- Asad F, Zhu HF, Zhang H, Liang EY, Muhammad S, Farhan SB, Hussain I, Wazir MA, Ahmed M, Esper J (2016) Are Karakoram temperatures out of phase compared to hemispheric trends? *Clim Dyn* 48(9–10):3381–3390
- Bao G, Liu Y, Liu N (2012) A tree-ring-based reconstruction of the Yimin river annual runoff in the Hulun Buir region, Inner Mongolia, for the past 135 years. *Chin Sci Bull* 57(36):4765–4775
- Chen F, Yu SL, Yuan YJ, Wang HQ, Gagen M (2016) A tree-ring width based drought reconstruction for southeastern China, links to Pacific Ocean climate variability. *Boreas* 45(2):335–346
- Chen F, Shang HM, Panyushkina I, Meko D, Li JB, Yuan YJ, Yu SL, Chen FH, He DM, Luo X (2019) 500-year tree-ring reconstruction of Salween river streamflow related to the history of water supply in Southeast Asia. *Clim Dyn* 53:6595–6607
- Classen AT, Sundqvist MK, Henning JA, Newman GS, Moore JAM, Cregger MA, Moorhead LC, Patterson CM (2015) Direct and indirect effects of climate change on soil microbial and soil microbial-plant interactions: what lies ahead? *Ecosphere* 6:1–21
- Cook ER, Holmes RL (1986) User's manual for ARSTAN. Laboratory of Tree-ring Research, University of Arizona, Tucson
- Cook ER, Kairiukstis LA (1990) Methods of dendrochronology. Kluwer Academic Publishers, Dordrecht
- Cook ER, Peters K (1997) Calculating unbiased tree-ring indices for the study of climatic and environmental change. *The Holocene* 7(3):361–370
- Cook ER, Anchukaitis KJ, Buckley BM, D'Arrigo RD, Jacoby GC, Wright WE (2010) Asian monsoon failure and Megadrought during the last millennium. *Science* 328(5977):486–489
- Davi NK, D'Arrigo R, Jacoby GC, Cook ER, Anchukaitis KJ, Nachin B, Rao MP, Leland C (2015) A long-term context (931–2005 C.E.) for rapid warming over Central Asia. *Quat Sci Rev* 121:89–97
- Deng Y, Gou XH, Gao LL, Zhang F, Xu X, Yang MX (2016) Tree-ring recorded drought variability in the northern Min Mountains of northwestern China. *Int J Clim* 36(10):3550–3560
- Deng Y, Gou XH, Gao LL, Yang MX, Zhang F (2017) Spatiotemporal drought variability of the eastern Tibetan Plateau during the last millennium. *Clim Dyn* 49(5–6):2077–2091
- Deslauriers A, Morin H, Begin Y (2003) Cellular phenology of annual ring formation of *Abies balsamea* in the Quebec boreal forest (Canada). *Can J for Res* 33:190–200
- Duan JP, Wang LL, Li L, Chen K (2010) Temperature variability since AD 1837 inferred from tree-ring maximum density of *Abies fabri* on Gongga Mountain, China. *Chin Sci Bull* 55:3015–3022
- Esper J, Cook ER, Schweingruber FH (2002) Low-frequency signals in long tree-ring chronologies for reconstructing past temperature variability. *Science* 295(5563):2250–2253
- Fan ZX, Brauning A, Fu PL, Yang RQ, Qi JH, Griebinger J, Gebrekirstos A (2019) Intra-annual radial growth of *Pinus kesiya*

- var. langbianensis* is mainly controlled by moisture availability in the Ailao Mountains Southwestern China. *Forests* 10:899
- Fang KY, Chen DL, Li JB, Seppä H (2014) Covarying hydroclimate patterns between monsoonal Asia and North America over the past 600 years. *J Clim* 27:8017–8033
- Fang KY, Guo ZT, Chen DL, Linderholm HW, Li JB, Zhou FF, Guo GY, Dong ZP, Li YJ (2017) Drought variation of western Chinese Loess Plateau since 1568 and its linkages with droughts in western North America. *Clim Dyn* 49:3839–3850
- Fritts HC (1976) *Tree rings and climate*. Academic Press, New York
- Gou XH, Chen FH, Jacoby G, Cook E, Yang MX, Peng JF, Zhang Y (2007) Rapid tree growth with respect to the last 400 years in response to climate warming, northeastern Tibetan Plateau. *Int J Climatol* 27:1497–1503
- Gou XH, Yang T, Gao LL, Deng Y, Yang MX, Chen FH (2013) A 457-year reconstruction of precipitation in the southeastern Qinghai-Tibet Plateau, China using tree-ring records. *Chin Sci Bull* 58(10):1107–1114 (in Chinese)
- Harris I, Osborn TJ, Jones P, Lister D (2020) Version 4 of the CRU TS monthly high-resolution gridded multivariate climate dataset. *Sci Data* 7:109
- He MH, Yang B, Datsenko NM (2014) A six hundred-year annual minimum temperature history for the central Tibetan Plateau derived from tree-ring width series. *Clim Dyn* 43:641–655
- Holmes RL (1983) Computer-assisted quality control in tree-ring dating and measurement. *Tree-Ring Res* 43:69–78
- Hu JH, Zeng H (2003) A preliminary analysis of stereoscopic exploitation and utilization of climate resources in central eastern Tibetan Plateau. *Chin J Agrometeorol* 24(1):54–57 (in Chinese)
- Huang R, Zhu HF, Liang EY, Liu B, Shi JF, Zhang RB, Yuan YJ, Griessinger J (2019) A tree ring-based winter temperature reconstruction for the southeastern Tibetan Plateau since 1340 CE. *Clim Dyn* 53(5–6):3221–3233
- IPCC (2021) In: *Climate change 2021: the physical science basis. Contribution of working group I to the sixth assessment report of the intergovernmental panel on climate CM-D*, V. Zhai P, Pirani A, Connors SL, Péan C, Berger S, Caud N, Chen Y, Goldfarb L, Gomis MI et al. (eds) Cambridge University Press, Cambridge, UK; New York, USA
- Jiao L, Wang SJ, Chen K, Liu XP (2022) Dynamic response to climate change in the radial growth of *Picea schrenkiana* in western Tien Shan, China. *J for Res* 33:147–157
- Körner C (1999) *Alpine plant life: functional plant ecology of high mountain ecosystems*. Springer, Berlin
- Li T, Li JB (2017) A 564-year annual minimum temperature reconstruction for the east central Tibetan Plateau from tree rings. *Glob Planet Change* 157:165–173
- Li JB, Xie SP, Cook ER (2014a) El Niño phases embedded in Asian and North American drought reconstructions. *Quat Sci Rev* 85:20–34
- Li JJ, Shao XM, Li YY, Qin NS (2014b) Annual temperature recorded in tree-ring from Songpan region. *Chin Sci Bull* 59:1446–1458
- Li ZS, Liu GH, Wu X, Gong L, Wang M, Wang XC (2015a) Tree ring-based temperature reconstruction over the past 186 years for the Miyaluo Natural Reserve, western Sichuan Province of China. *Theor Appl Climatol* 120(3–4):495–506
- Li ZS, Liu GH, Wu X, Wang XC (2015b) Tree-ring-based temperature reconstruction for the Wolong Natural Reserve, central eastern Tibetan Plateau of China. *Int J Climatol* 35(11):3296–3307
- Li JB, Shi JF, Zhang DD, Yang B, Fang KY, Yue PH (2017) Moisture increase in response to high-altitude warming evidenced by tree-rings on the southeastern Tibetan Plateau. *Clim Dyn* 48(1–2):649–660
- Li JX, Li JB, Li T, Au TF (2021) 351-year tree ring reconstruction of the Gongga Mountains winter minimum temperature and its relationship with the Atlantic multidecadal oscillation. *Clim Change* 165:49
- Liang EY, Shao X, Xu Y (2009) Tree-ring evidence of recent abnormal warming on the southeast Tibetan plateau. *Theor Appl Climatol* 98(1–2):9–18
- Liang HX, Lyu LX, Wahab M (2016) A 382-year reconstruction of August mean minimum temperature from tree-ring maximum latewood density on the southeastern Tibetan Plateau, China. *Dendrochronologia* 37:1–8
- Liu Y, An ZS, Linderholm HW, Chen DL, Song HM, Cai QF, Sun JY, Tian H (2009) Annual temperatures during the last 2485 years in the mid-eastern Tibetan Plateau inferred from tree rings. *Sci China Ser D* 52(3):348–359
- Liu Y, Cobb KM, Song HM, Li Q, Li CY, Nakatsuka T, An ZS, Zhou WJ, Cai QF, Li JB, Leavitt SW, Sun CF, Mei RC, Shen CC, Chan MH, Sun JY, Yan LB, Lei Y, Ma YY, Li XX, Chen DL, Linderholm HW (2017a) Recent enhancement of central Pacific El Niño variability relative to last eight centuries. *Nat Commun* 8:15386
- Liu Y, Liu H, Song HM, Li Q, Burr GS, Wang L, Hu SL (2017b) A monsoon-related 174-year relative humidity record from tree-ring $\delta^{18}\text{O}$ in the Yaoshan region, eastern central China. *Sci Total Environ* 593–594:523–534
- Mann ME, Lees JM (1996) Robust estimation of background noise and signal detection in climatic time series. *Clim Change* 33:409–445
- Mann ME, Zhang ZH, Hughes MK, Bradley RS, Miller SK, Rutherford S, Ni FB (2008) Proxy-based reconstructions of hemispheric and global surface temperature variations over the past two millennia. *P Natl Acad Sci USA* 105(36):13252–13257
- Michaelsen J (1987) Cross-validation in statistical climate forecast models. *J Clim Appl Meteor* 26:1589–1600
- Peng JF, Liu YZ (2013) Reconstructed droughts for the northeastern Tibetan Plateau since AD 1411 year and its linkages to the Pacific, Indian and Atlantic Oceans. *Quat Int* 283:98–116
- Rayner NA, Parker DE, Horton EB, Folland CK, Alexander LV, Rowell DP, Kent EC, Kaplan A (2003) Global analyses of sea surface temperature, sea ice, and night marine air temperature since the late nineteenth century. *J Geophys Res* 108:D144407
- Shao XM, Fan JM (1999) Past climate on west Sichuan Plateau as reconstructed from ring-widths of dragon spruce. *Quat Sci* 19:81–89 (in Chinese)
- Shao XM, Huang L, Liu HB, Liang EY, Fang XQ, Wang LL (2005) Reconstruction of precipitation variation from tree rings in recent 1000 years in Delingha, Qinghai. *Sci Chin Ser D* 48(7):939–949
- Shao X, Xu Y, Yin ZY, Liang E, Zhu H, Wang S (2010) Climatic implications of a 3585-year tree-ring width chronology from the northeastern Qinghai-Tibetan Plateau. *Quat Sci Rev* 29:2111–2122
- Shi JF, Li JB, Zhang DD, Zheng JY, Shi SY, Ge QS, Lee HF, Zhao YS, Zhang J, Lu HY (2017) Two centuries of April–July temperature change in eastern China and its influence on grain productivity. *Sci Bull* 62:40–45
- Shi CM, Masson-Delmotte V, Daux V, Li ZS, Carré M, Moore JC (2015) Unprecedented recent warming rate and temperature variability over the east Tibetan Plateau inferred from Alpine treeline dendrochronology. *Clim Dyn* 45(5–6):1367–1380
- Song HM, Liu Y, Ni W, Cai QF, Sun JY, Ge W, Xiao W (2007) Winter mean lowest temperature derived from tree-ring width in Jiuzhaigou region, China since 1750 AD. *Quat Sci* 27(4):486–491
- Stokes MA, Smiley TL (1968) *Introduction to tree-ring dating*. University of Chicago Press, Chicago
- Sun CF, Liu Y, Song HM, Cai QF, Li Q, Wang L, Mei RC, Fang CX (2018) Sunshine duration reconstruction in the southeastern

- Tibetan plateau based on tree-ring width and its relationship to volcanic eruptions. *Sci Total Environ* 628–629:707–714
- Torrence C, Compo GP (1998) A practical guide to wavelet analysis. *B Am Meteorol Soc* 79:61–78
- Wang HL, Shao XM, Li MQ (2019) A 2917-year tree-ring-based reconstruction of precipitation for the Buerhanbuda Mts., South-eastern Qaidam Basin, China. *Dendrochronologia* 55:80–92
- Wigley T, Briffa KR, Jones PD (1984) On the average value of correlated time-series, with applications in dendroclimatology and hydrometeorology. *J Clim Appl Meteorol* 23:201–213
- Wilson R, Anchukaiti K, Briffa KR, Büntgen U, Cook E, D'Arrigo R, Davi N, Esper J, Frank D, Gunnarson B, Hegerl G, Helama S, Klesse S, Krusic PJ, Linderholm HW, Myglan V, Osborn TJ, Rydval M, Schneider L, Schurer A, Zorita E (2016) Last millennium northern hemisphere summer temperatures from tree rings, part I, the long term context. *Quat Sci Rev* 134:1–18
- Wu P, Wang LL, Shao XM (2005) Reconstruction of summer temperature from maximum latewood density of *Pinus densata* in west Sichuan. *Acta Geogr Sin* 60(6):998–1006 (in Chinese)
- Xiao DM, Qin NS, Huang X (2015) A 325-year reconstruction of July–August mean temperature in the north of west Sichuan derived from tree-ring. *Quat Sci* 35:1134–1144 (in Chinese)
- Yang B, Qin C, Wang JL, He MH, Melvin TM, Osborn TJ, Briffa KR (2014) A 3500-year tree-ring record of annual precipitation on the northeastern Tibetan Plateau. *Proc Natl Acad Sci USA* 111:2903–2908
- Yang B, Sonechkin D, Datsenko N, Liu JJ, Qin C (2017) Establishment of a 4650-year-long eigenvalue chronology based on tree-ring cores from Qilian junipers (*Juniperus przewalskii* Kom) in Western China. *Dendrochronologia* 46:56–66
- Yin H, Liu HB, Linderholm HW, Sun Y (2015) Tree ring density-based warm-season temperature reconstruction since A.D. 1610 in the eastern Tibetan Plateau. *Palaeogeogr Palaeoclimatol Palaeoecol* 426:112–120
- Yu J, Liu Q (2020) *Larix olgensis* growth-climate response between lower and upper elevation limits: an intensive study along the eastern slope of the Changbai Mountains, northeastern China. *J for Res* 31:231–244
- Yu SL, Yuan YJ, Wei WS, Zhang TW, Shang HM, Chen F (2012) Reconstructed mean temperature in Mearkang, West Sichuan in July and its detection of climatic period signal. *Plateau Meteorol* 31:193–200 (in Chinese)
- Zhang ZH (2015) Tree-rings, a key ecological indicator of environment and climate change. *Ecol Indic* 51:107–116
- Zhang TW, Yuan YJ, Wei WS, Yu SL, Zhang RB, Chen F, Shang HM, Qin L (2014a) A tree-ring based precipitation reconstruction for the Mohe region in the northern Greater Hignnan Mountains, China, since AD 1724. *Quat Res* 82(1):14–21
- Zhang Y, Shao XM, Yin ZY, Wang Y (2014b) Millennial minimum temperature variations in the Qilian Mountains, China: evidence from tree rings. *Clim past* 10:1763–1778
- Zhang QB, Evans MN, Lyu LX (2015) Moisture dipole over the Tibetan Plateau during the past five and a half centuries. *Nat Commun* 6:8062
- Zhang RB, Wei WS, Shang HM, Yu SL, Gou XH, Qin L, Bolatov K, Mambetov BT (2019) A tree ring-based record of annual mass balance changes for the TS. Tuyuksuyskiy Glacier and its linkages to climate change in the Tianshan Mountains. *Quat Sci Rev* 205:10–21
- Zhang XL, Li JX, Liu XB, Chen ZJ (2020) Improved EEMD-based standardization method for developing long tree-ring chronologies. *J for Res* 31:2217–2224
- Zhu LJ, Zhang YD, Li ZS, Guo BD, Wang XC (2016) A 368-year maximum temperature reconstruction based on tree-ring data in the northcentral eastern Tibetan Plateau Plateau (NWSP), China. *Clim past* 12:1485–1498

Publisher's Note Springer Nature remains neutral with regard to jurisdictional claims in published maps and institutional affiliations.